

Oscillatory behavior and anomalous heat evolution in recombination of H₂ and O₂ on Pd-based catalysts

Erwin Lalik, A Drelinkiewicz, Robert Kosydar, Tomasz Szumelda, Elzbieta Bielanska, Dan Groszek, Angelo Iannetelli, and Martin Groszek

Ind. Eng. Chem. Res., **Just Accepted Manuscript** • Publication Date (Web): 29 Jun 2015

Downloaded from <http://pubs.acs.org> on June 30, 2015

Just Accepted

"Just Accepted" manuscripts have been peer-reviewed and accepted for publication. They are posted online prior to technical editing, formatting for publication and author proofing. The American Chemical Society provides "Just Accepted" as a free service to the research community to expedite the dissemination of scientific material as soon as possible after acceptance. "Just Accepted" manuscripts appear in full in PDF format accompanied by an HTML abstract. "Just Accepted" manuscripts have been fully peer reviewed, but should not be considered the official version of record. They are accessible to all readers and citable by the Digital Object Identifier (DOI®). "Just Accepted" is an optional service offered to authors. Therefore, the "Just Accepted" Web site may not include all articles that will be published in the journal. After a manuscript is technically edited and formatted, it will be removed from the "Just Accepted" Web site and published as an ASAP article. Note that technical editing may introduce minor changes to the manuscript text and/or graphics which could affect content, and all legal disclaimers and ethical guidelines that apply to the journal pertain. ACS cannot be held responsible for errors or consequences arising from the use of information contained in these "Just Accepted" manuscripts.



Oscillatory behavior and anomalous heat evolution in recombination of H₂ and O₂ on Pd-based catalysts

Erwin Lalik^{a}, Alicja Drelinkiewicz^a, Robert Kosydar^a, Tomasz Szumelda^a, Elżbieta Bielańska^a,
Dan Groszek^b, Angelo Iannetelli^b, Martin Groszek^b*

a) Jerzy Haber Institute of Catalysis and Surface Chemistry, Polish Academy of Science, ul.
Niezapominajek 8, Krakow 30-239, Poland; **b)** Microscal Energy Technology Ltd., 188
Greenham Business Park, Thatcham, RG19 6HW, UK;

ABSTRACT: Gas flow-through microcalorimetry has been applied to study the Pd/Al₂O₃ type catalysts in the exothermic hydrogen recombination process: H₂ + O₂ → H₂O, in view of the potential application in the passive autocatalytic recombination (PAR) technology. The flow mode experiments revealed thermokinetic oscillations, i.e., the oscillatory rate of heat evolution accompanying the process and the corresponding oscillations in the differential heat of process, in sync with oscillatory conversion of hydrogen. Mathematical evidence has been found for deterministic character of the aperiodic oscillations. In the outburst of quasiperiodic oscillations of large amplitude, the instances of differential heats as high as 700 kJ/mol H₂ have been detected, exceeding the heat of the gaseous water formation from elements (242 kJ/mol H₂) by a factor of nearly three. Another occurrence of anomalously high thermal effects has been

measured in calorimetric oxygen titration using 0.09 μmol pulses of O_2 injected onto hydrogen- or deuterium-saturated catalysts, including 2%Pd/ Al_2O_3 , 5%Pd/ Al_2O_3 and 2%PdAu/ Al_2O_3 . Repeatedly, the saturation/oxidation cycles showed the heat evolutions in certain individual O_2 pulses as high as 1100 kJ/mol O_2 , i.e., 550 kJ/mol H_2 , again twice as much as the heat of water formation. It has been pointed out that it seems prudent for the PAR technologists to assume a much larger rate of heat evolution than those calculated on the basis of a standard thermodynamic value of the heat of water formation, in order to account for the possibility of large thermokinetic oscillation occasionally appearing in the recombination process of hydrogen. A possible relation of the anomalous heat evolution to an inadvertent occurrence of low energy nuclear reaction (LENR) phenomena is also briefly considered.

1. INTRODUCTION.

In designing nuclear reactors, safety must be kept uppermost in one's mind and prominent among the safety issues is that of hydrogen safety. Due to various adverse processes, the water that is used as a cooling medium within the reactor confinement can also be a source of gaseous hydrogen. The latter's concentration, if it is accumulated in an uncontrolled manner, may easily reach an explosive limit in a mixture with air. A hydrogen explosion is therefore a threat which, due to the fact that it may take place in a close vicinity to the nuclear core, can have potentially disastrous consequences, including an uncontrollable release of radioactive material.

To mitigate the hazard posed by hydrogen, passive autocatalytic recombiners (PARs) are widely applied in nuclear reactors as a remedy. In spite of the name, the recombination reaction of $\text{H}_2 + \text{O}_2 \rightarrow \text{H}_2\text{O}$, which proceeds within the PAR, is not truly an autocatalytic one. It requires

a solid catalyst for the recombination to occur at a moderate temperature, and supported noble metals (Pd, Pt) are mostly used for this purpose.¹⁻⁴

The idea behind the PAR design is that it should work reliably without constant human control, and crucially, without an external energy source such as electricity, since in case of an accident, such factors might well be expected to fail. The catalytic recombination of H₂ and O₂ should be, therefore, ideally left to its own means in the task of prevention of hydrogen gas accumulation. However, complexity of the reaction mechanism and energetics will have a bearing on effectiveness of PAR technology. The formation of water is a highly exothermic reaction ($\Delta H^\circ(298.15\text{ K}) = -242\text{ kJ/mol H}_2$ for H₂O_g formation from elements⁵), and so a potentially high rate of heat evolution must be carefully considered in effective PAR design. Currently, this is addressed by assuming a twofold role played by natural convection. Apart from the removal of the evolving heat, it is also supposed to ensure an efficient gas circulation within the PAR interior. This assumes that the heat evolution in this reaction is “well-behaved”.

But there are hints that the system may behave in a less than predictable manner. In fact, the reaction is known to have rather intricate kinetics. It is capable of attaining multiple steady states^{6,7}, a trait it shares with other Pd-catalyzed reactions. The notoriously evasive hysteretic phenomena, in other words multiple steady states in the metallic Pd catalysis, may not be featured often in literature, but are a frequent subject of conversations among scientists working in the field. The metal-catalyzed reaction is also capable of reaching oscillatory regime(s). The oscillatory kinetics in the hydrogen oxidation have been reported on palladium,^{8,9} platinum,¹⁰⁻¹² and nickel,¹³⁻¹⁸ i.e., on the metals that are also known for dissociative sorption of H₂. Although oscillatory oxidation of H₂ on Pd is not studied very often, metallic Pd is by no means a stranger in oscillatory catalysis. In fact, oscillatory oxidations of CO on metallic Pd or Pt are classic

systems widely studied for their nonlinear dynamics,¹⁹⁻²⁴ also leading to the Nobel Prize in chemistry in 2007. As for the H/Pd system, a handful of results on oscillatory hydrogenations have been published.^{25,26} Thermokinetic oscillations in the Pd/H system, i.e., the oscillatory rate of heat evolution accompanying the sorption of hydrogen and/or deuterium in metallic palladium have been reported recently.²⁷⁻²⁹ Moreover, an incidence of anomalously high thermal effects has been observed in the H₂/O₂/Pd system, as well as in the H₂/O₂/Ni, and also with noble metals catalysts such as Au/TiO₂, considerably exceeding the thermodynamically expected heat of water formation.³⁰⁻³²

Here we use the gas flow-through microcalorimetric method to detect both the thermokinetic oscillations as well as anomalous heat evolutions in the catalytic recombination of H₂ and O₂ on the Pd supported catalysts, including 2%Pd/Al₂O₃, 5%Pd/Al₂O₃ and PdAu/Al₂O₃, i.e. of the type usually applied in the PARs. We show that instantaneous thermal effects as high as 700 kJ/mol H₂ which is nearly three times as much as the “normal” heat of water formation, may unexpectedly appear in this reaction. We believe that those findings are important for the hydrogen safety of nuclear reactors, and that heat evolutions much larger than the thermodynamic values of 242 kJ/mol H₂ should be considered in the PAR design proceedings.

2. EXPERIMENTAL

2.1. Materials. The high purity gases were provided by Linde Gaz Poland S.A.. Hydrogen, nitrogen and oxygen gases were of purity 99.999 % vol., and deuterium gas of purity 99.9 % vol.. The synthetic air contained 80 % vol. of N₂ plus 20 % vol. O₂. The 5%Pd/Al₂O₃ catalyst has been provided by Alfa Aesar. The synthesis of the 2%Pd/Al₂O₃ and 2%PdAu/Al₂O₃ catalysts has been described in the next subsection.

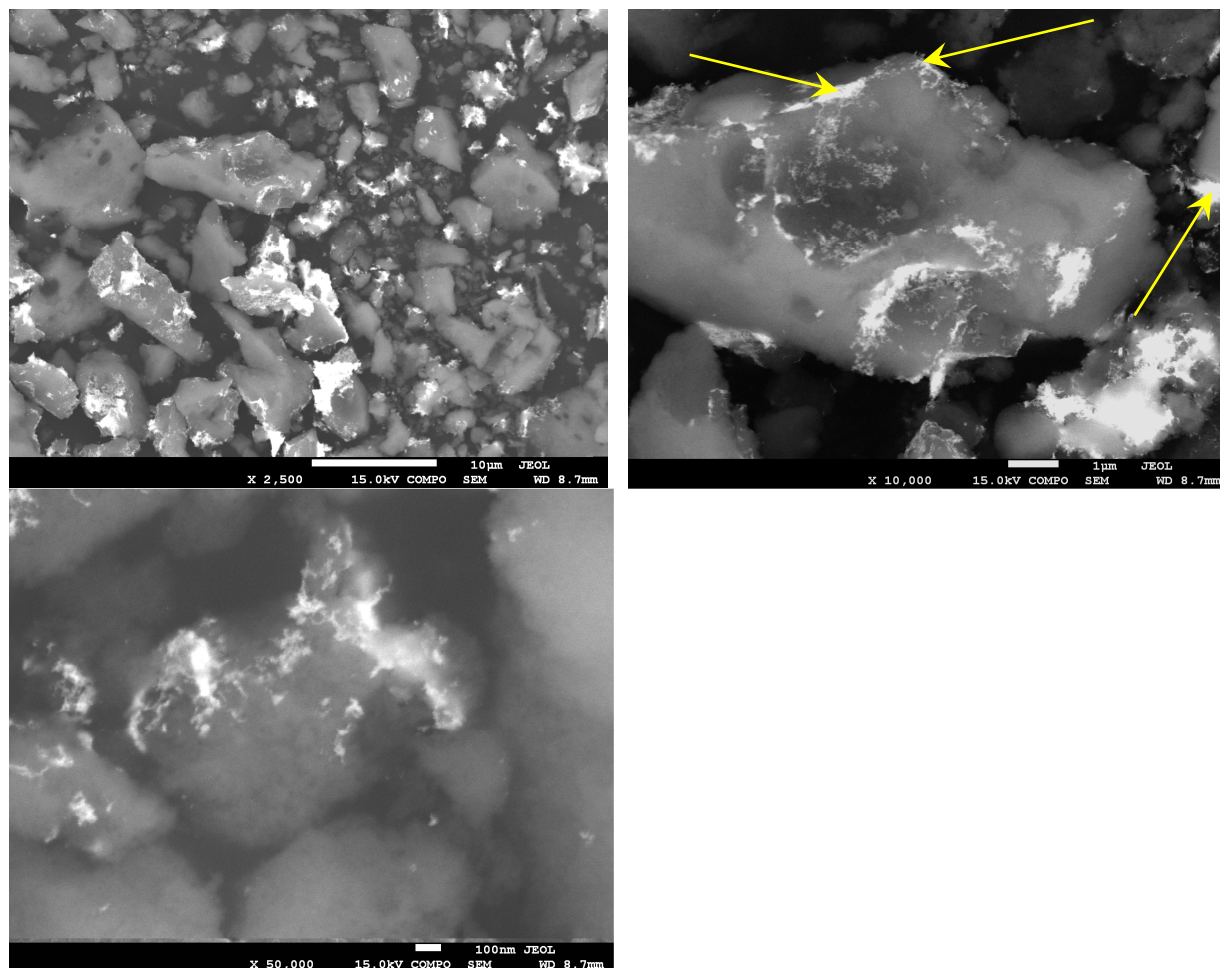


Figure 1. The bright areas in the SEM images represent the alloyed Pd-Au nanoparticles of the 2%PdAu/Al₂O₃ catalyst used for experiments described in section 3.4.4. Magnification, from left to right: 2,500×, 10,000×, and 50,000×, the white bars representing, respectively, 10 μm, 1 μm, 100 nm. The EDS measured Pd/Au atomic ratio values for the points marked with yellow arrows in the upper left panel are from left to right: 74/26, 77/23, 72/28, indicative of Pd and Au being distributed in even proportions among the bimetallic particles.

2.2. Preparation of catalysts. Alumina (γ - Al₂O₃, Procatalyse, surface area 200 m²/g, porosity 0.48 cm³/g, d = 9.3 nm) was used as the support. The 2%Pd/Al₂O₃ catalysts were prepared by reverse “water-in-oil” microemulsion method according to our previous

procedure.^{33,34} The reverse micellar solutions were prepared using polyoxyethylene(7-8) octylphenyl ether (Triton-X 114) (Aldrich) as the surfactant and cyclohexane (Aldrich) as the oil phase. The value of parameter W (water to surfactant molar ratio) equal to 5 was applied.

The aqueous solutions of PdCl_2 (molar ratio of $\text{NaCl} : \text{PdCl}_2 = 2$, Pd^{2+} ions concentration of 0.2 mol/dm^3 and HAuCl_4 (0.05 mol/dm^3) was used as precursors and hydrazine hydrate ($\text{N}_2\text{H}_4 \times \text{H}_2\text{O}$, N_2H_4 64-65 %, reagent grade 98 %, Aldrich) was used as reducing agent.

A solution of PdCl_2 or a mixture of $\text{PdCl}_2 - \text{HAuCl}_4$ aqueous solutions were introduced to cyclohexane-surfactant solution and the obtained suspension was vigorously stirred up to the formation of transparent, clear dark orange solution. The hydrazine (64 - 65 %) was added directly to the microemulsion (hydrazine to metal ions molar ratio of 20). The reduction of metal ions was a fast process and the color of liquid quickly changed to black. Stirring was then continued for another 1 h. After this period the support Al_2O_3 was introduced and stirring was continued for another 1 h. Deposition of metal nanoparticles on the support was carried out by slow adding the THF solvent, with the solution vigorously stirred. The volume of the THF added was 3-4 times the volume of the microemulsion. Upon addition of THF, the colour of liquid gradually changed from black to colorless, indicative of complete deposition of metal particles on the support. The obtained catalyst was separated by filtration, dried in air for ca. 24 h, and washed with a copious amount of methanol and acetone. Finally, the catalysts were washed with water up to the removal of chloride ions, dried overnight in air and then calcined at 120°C for 16 h. The SEM images in Figure 1 show the characteristic cloud-like shaped agglomerations of metallic particles located on the Al_2O_3 grains typically obtained in the described method.

Electron Microscopy (SEM, TEM) studies were performed by means of Field Emission Scanning Electron Microscope JEOL JSM – 7500 F equipped with the X-ray energy dispersive (EDS) system. Two detectors were used and the images were recorded in two modes. The secondary electron detector provided SEI images, and back scattered electron detector provided BSE (COMPO) micrographs.

2.3. Microcalorimetry. *2.3.1. General.* Microcalorimetric experiments were performed using Microscal FMC 4110 microcalorimeter. The design and operation of this instrument have been described in detail in Ref. 35. The instrument measures the rate of heat evolution accompanying a solid-gas interaction. A sample of catalyst is placed in a small microcalorimetric cell (7 mm in diameter), and the measurement is carried out in flow-through mode. The cell is placed centrally within a much larger, metal block acting as a heat sink. The latter ensures a steady removal of total evolving heat, thus preventing its accumulation within the cell. The heat sink has to be large enough for its outer edge to be sufficiently far away from the cell so as not to sense the rising temperature. Hence, as a reaction is occurring within the cell, a minute difference of temperatures between the close vicinity of the cell and the edge of the heat sink can be measured continuously by a system of thermistors appropriately located within the block. The calorimetric signal from the thermistors can be converted into the representation of the rate of heat evolution using a calibration factor extracted for each experiment by *in situ* calibration pulse produced by calibrator located axially within the cell. The FMC microcalorimeter is also equipped with the downstream detector (DSD), currently a thermal conductivity detector (TCD), to analyze the H₂ concentration after the recombination process. The rate of consumption of H₂ is, therefore, determined concurrently with the rate of heat evolution, which is necessary to calculate both the enthalpy of process and the conversion of H₂.

2.3.2. *Safety.* The lack of heat cumulation within the very small cell (0.15 cm^3) effectively eliminates the danger of thermal explosion of the H_2/O_2 mixture, thus making the instrument suitable for measuring thermal effects of the oxidation of hydrogen at various proportions of H_2/O_2 . To obtain various H_2 concentration, two mass flow controllers (Bronkhorst) and a system of valves made it possible to mix the H_2 with synthetic air at various proportions prior to their reaching the cell, as well as to establish the mixture's flow rate. On its way from the manifold, the reaction mixture is passing through the feed tubing of 0.04" (1.016 mm) ID, which is safe against a homogeneous ignition.³⁶

2.3.4. *Error estimation.* Error estimation for the microcalorimetric measurements has been attempted in Ref. 28 basing on 50 sorption/desorption cycles of hydrogen or deuterium in metallic palladium powder. The data has been represented as a function of H_2 or D_2 partial pressure, separately for the heats of sorption and desorption. Since the range of hydrogen partial pressure variability was very narrow, it has been assumed that both the heat of sorption and the heat of desorption could be a linear function of the hydrogen content in reaction mixture. The scatter of the experimental values around their fitted straight lines has been then taken as representing an experimental error. Using the absolute relative difference formula, the estimated error has been found to range between 1.42 % and 1.86 %, and it has been concluded that the error in determining the heat evolution in sorption/desorption cycles of hydrogen in Pd was less than 2 %.

2.3.5. *Calorimetric procedures.* Both the flow-mode and the pulse-mode (calorimetric titration) experiments were carried out at room temperature ($22 \text{ }^\circ\text{C}$ - $23 \text{ }^\circ\text{C}$) and under the atmospheric pressure. In the flow-mode experiments, a reaction mixture of H_2 concentration 6.2, 7.2 or 8.6 vol.% in synthetic air (20% O_2 + 80 % N_2) was used, with the flow rates $6.7 \text{ cm}^3/\text{min}$

7.0 cm³/min and 7.5 cm³/min, respectively, corresponding to residence times of 1.34 s, 1.28 s and 1.20 s (cell volume 0.15 cm³). For each concentration setup, the reaction was carried out for a period of ca. 1 h. The amount of the catalyst used to fill the cell ranged from 0.14 g to 0.17 g. Prior to experiment, the catalyst was pretreated *in situ* with pure hydrogen at 100 °C for 4 h. In the pulse-mode experiments, the N₂ gas is used as carrier and a 10 mm³ gas loop as dosing device to produce pulses of either synthetic air (0.09 μmol O₂) or pure oxygen (0.46 μmol O₂).

3. RESULTS.

3.1. The occurrence of oscillations in flow-mode recombination of H₂ + O₂. Figures 2 and 3 show the outbursts of thermokinetic oscillations triggered by a change in concentration of H₂ in reaction mixture, recorded with the gas flow-through microcalorimeter loaded with the 2%Pd/Al₂O₃ catalyst. Figure 2 shows the process on the fresh catalyst, while the results in Figure 3 represents an analogous experiment carried out on the same catalyst preheated at 150 °C for 4 h in nitrogen flow. The rate of heat evolution accompanying the H₂ + O₂ recombination is represented by the calorimetric curve (red) shown in the upper parts in both figures. The whole recombination experiment consists of three rounds, using different concentrations of H₂ in a mixture with synthetic air. The H₂ concentration was increased successively, from one round to the next, i.e., from 6.2 % in the first to 7.2 % and up to 8.6 % vol. of H₂ in the last round. The rounds are separated by a short gap in which the calorimetric cell is cut off for a short period, so that the calorimetric curve drops to zero, effectively yielding a separate exothermic peak for each setting of H₂ concentration. This makes it easier to calculate the total heat evolved for each round separately, by integrating the areas under the respective peaks. The uptake of H₂ is concurrently monitored by a down stream detector (TCD), and the TCD line (blue) represents the

rate of H_2 consumption as a function of time on stream. On integration, each of the blue peaks yields a total uptake of H_2 for a respective concentration. The ratio of areas under a calorimetric peak (pink) and its corresponding TCD peak (light blue) yields an average molar heat of the recombination process expressed in kJ/mol H_2 .

The thermokinetic oscillations are clearly visible in the calorimetric curves following the increasing of the H_2 concentration from 6.2 % to 7.2 % vol. in both figures (Figs. 1 and 2). In Figure 2, the outburst of seemingly periodic oscillations is a short-lived episode, but it is then followed by aperiodic oscillations towards the end of the 7.2 % round. On the other hand, the oscillations in the 7.2 % round in Figure 2 are quasiperiodic (cf. Fig. 4A) and of much larger amplitude, with the rate of heat evolution at the crests as high as 200 mW, and dropping nearly to zero at the troughs. The corresponding oscillations in the TCD curve are much less pronounced. Figure 4 represents enlarged fragments of both the calorimetric and the TCD curves showing their oscillatory dynamics. The fragments shown in Figures 4A and B represent the episodes of quasiperiodic oscillations, respectively, in the 7.2 % and the 8.6 % round of Figure 3. In both cases, the crests in the rate of heat evolution strictly coincide with dips in the hydrogen uptake rate, i.e.; both time series are anti-phase synchronized. The fragment in Figure 4C also comes from the 8.6 % round in Figure 3, but it represents aperiodic (chaotic) oscillations. In vivid contrast to the quasiperiodic dynamics, there is no obvious synchronization of heat evolution with hydrogen uptake in the course of aperiodic oscillations.

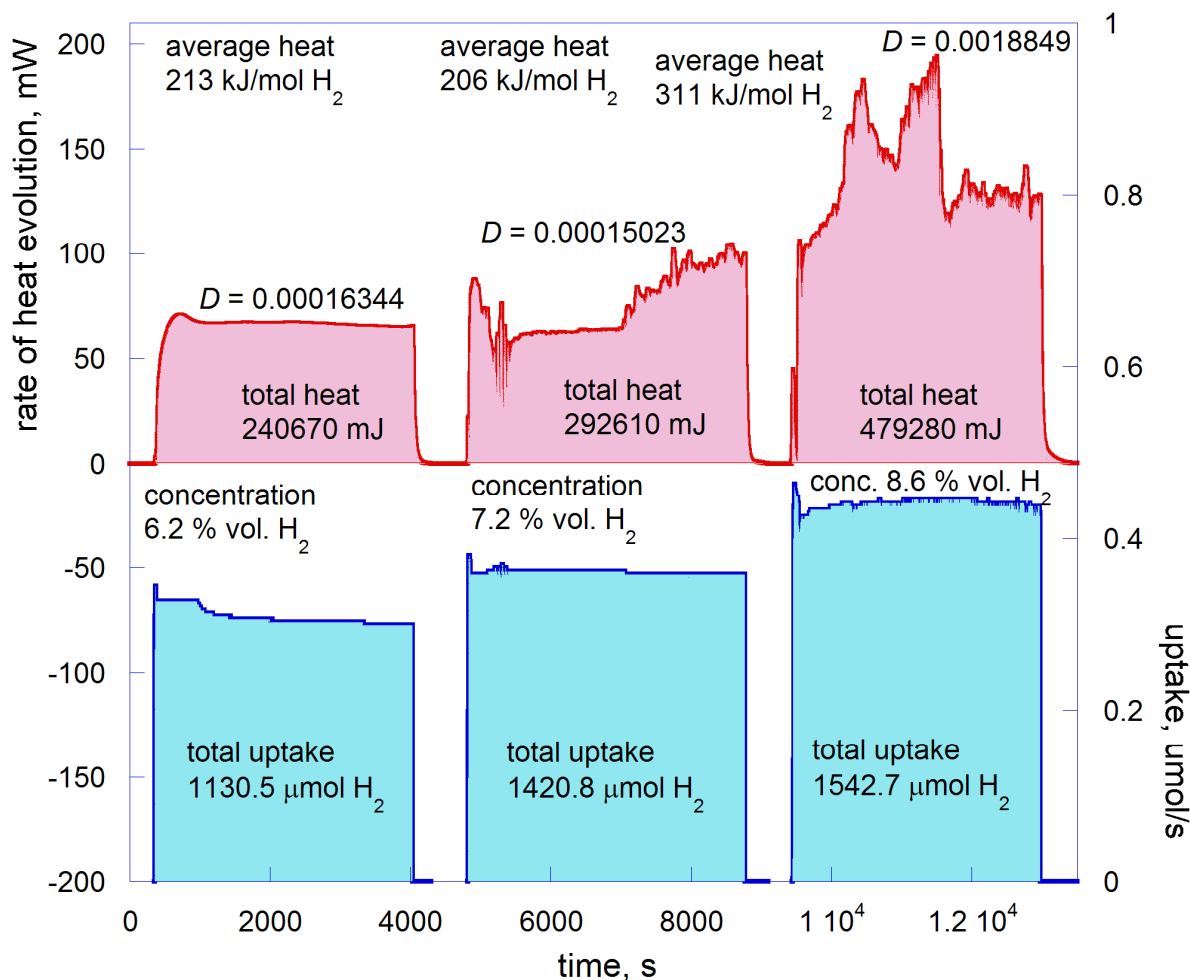


Figure 2. The heat of recombination of $\text{H}_2 + \text{O}_2$ (red) measured by gas-flow through microcalorimeter concurrently with the uptake of hydrogen (blue) for various H_2 concentrations on the 2%Pd/ Al_2O_3 catalyst. The areas under curves represent the total heats (magenta) and total uptake of hydrogen (light blue) for individual rounds; the ratio of the two yields the average molar heat of process for a round. The results of D -test are given for each round (cf. Section 3.2).

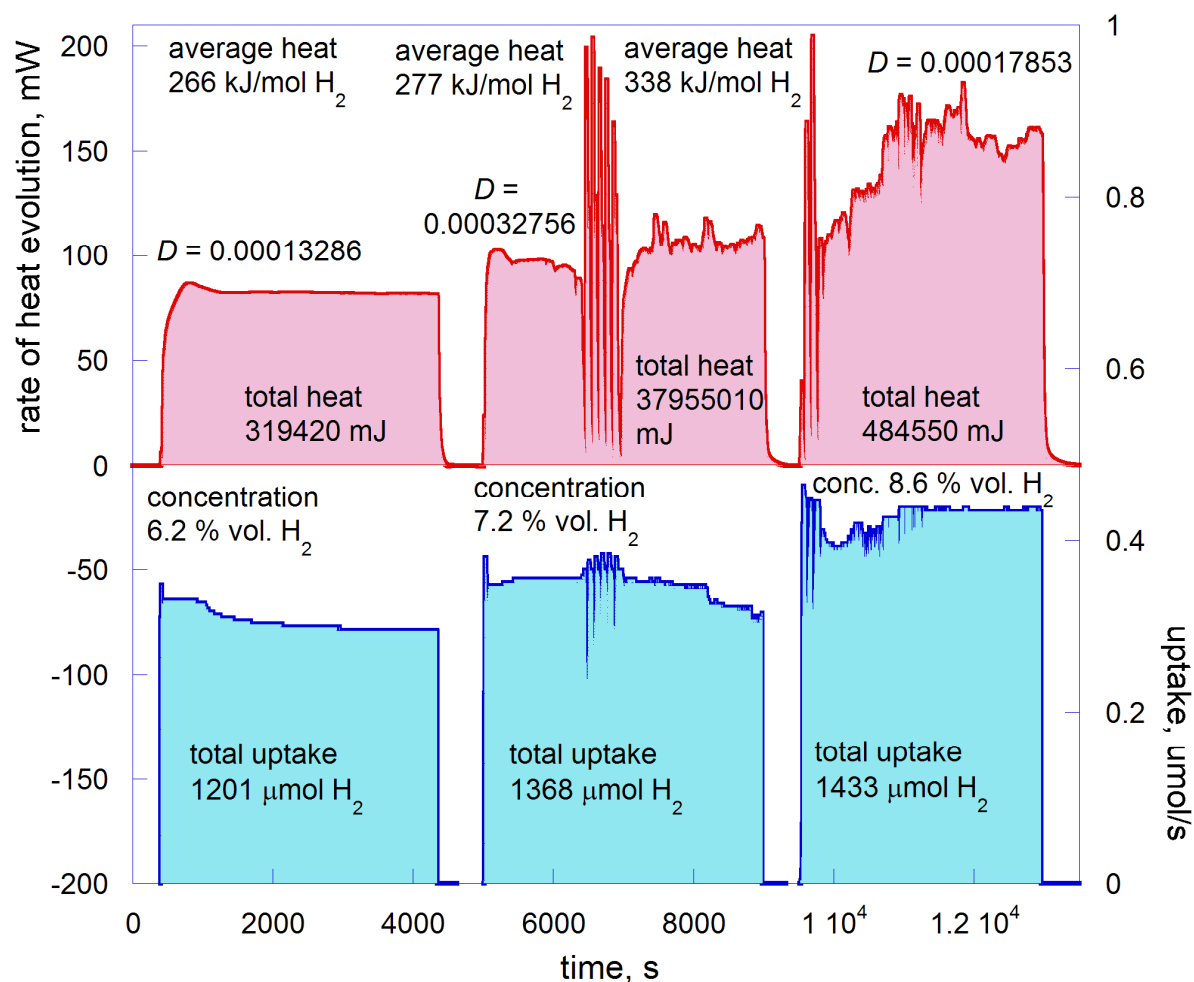


Figure 3. Repetition of experiment represented in Figure 2 following a heating of catalyst for 4 h at 150 °C in N₂. Note the outburst of large-amplitude oscillations in the middle of the 7.2 % round and at the beginning of the 8.6 % round.

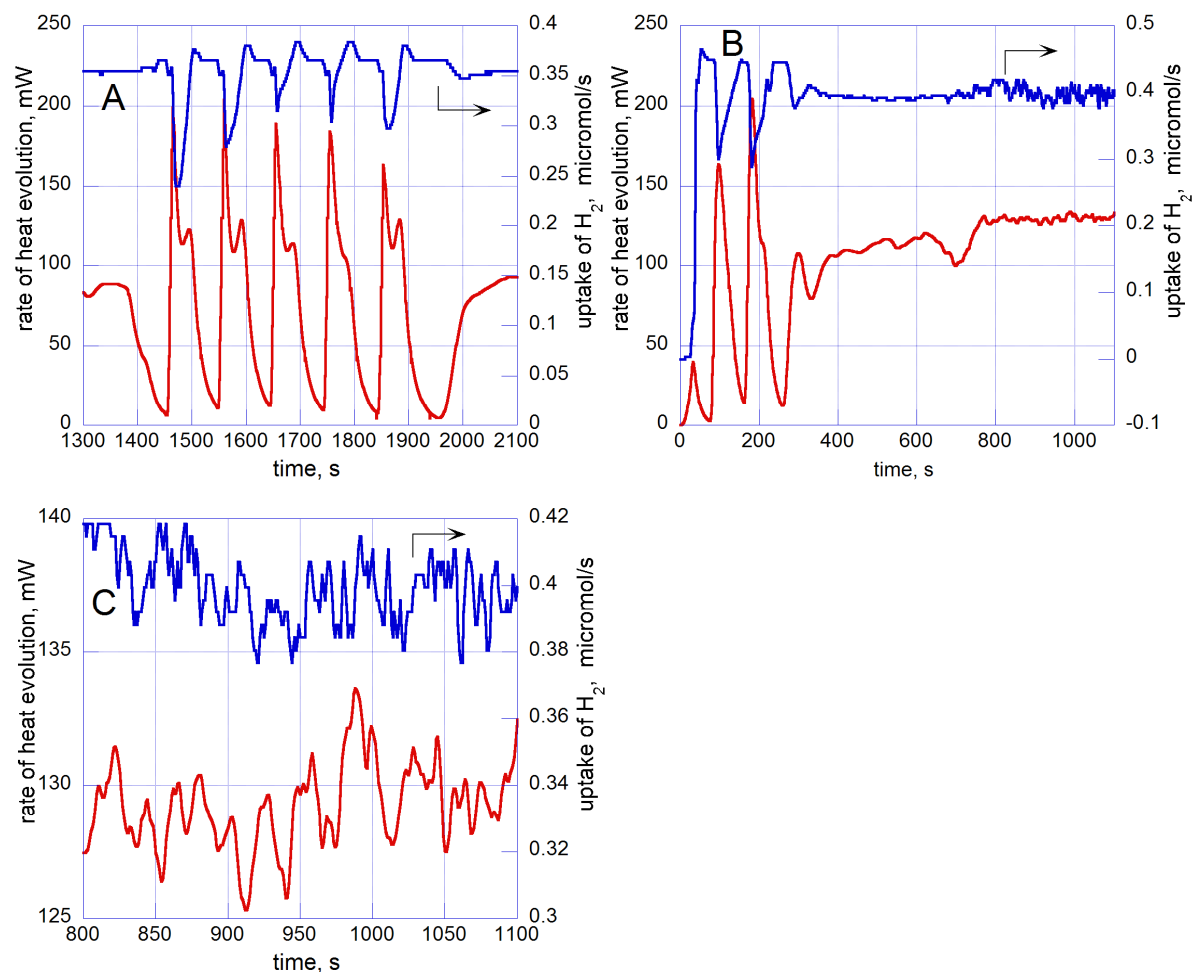


Figure 4. Dynamics of oscillatory oxidation of hydrogen on 2%Pd/Al₂O₃ catalyst. For quasiperiodic oscillations (**A** and **B**), the crests in the quasiperiodic oscillations of heat evolution rate (red line) strictly coincide with dips in the hydrogen uptake rate (blue line), but there is no obvious relation between the two rates during the aperiodic, chaotic oscillations (**C**). Represented here are enlarged fragments of experimental curves shown in Figure 3, i.e., the 7.2 % round (**A**) and the 8.6 % round (**B** and **C**), with Panel **C** showing still enlarged view of the part of Panel **B** between 800 s - 1100 s.

3.2. The *D*-testing for deterministic chaos. The *D*-test has been used to confirm deterministic character of the aperiodic oscillations that dominate the rounds for 7.2 % and 8.6 % concentrations of H₂ in Figures 2 and 3. This is to say, we need to determine that the aperiodic, calorimetric time series in Figures 2 and 3 are a manifestation of a reaction dynamics, and, therefore, that we observe a kinetic phenomenon of oscillating reaction rather than a stochastic noise of microcalorimetric recording. The underpinning mathematics as well as the testing procedure are described in detail in the Ref. 29, so they are only outlined here. Consider a function $f(x)$ which is smooth, continuous and square integrable on the interval $[a, b] \subset \mathbb{R}$. If the values of the function $f(x)$ are zero at the points a and b then the following relation holds (see Ref. 29 for proof of this relation):

$$-\int_a^b \left(\frac{d[f(x)]}{dx} \int_a^x f(t) dt \right) dx = \int_a^b [f(x)]^2 dx \quad (1)$$

The formula (1) compares two definite integrals. The integrand in the left hand side (LHS) represents a pointwise product, $p(x)$, of two functions, namely: the first derivative of $f(x)$ and the integral of $f(x)$ with the variable upper limit. The integrand in the right hand side (RHS) is the $f(x)$ squared. In other words, if the a and b are both zero crossings of $f(x)$, i.e., for $f(a) = f(b) = 0$, given that $f(x)$ is smooth, continuous and square integrable on the interval $[a, b]$, then the areas under the curves of the $[f(x)]^2$ and the $p(x)$, within the $[a, b]$, are equal to each other in absolute value but opposite in sign. Both sides of (1) represent a real number. For brevity, subsequently the letters P and S will be used to denote, respectively, the integrals in LHS and RHS of (1). Since S is always positive, then P must be negative, and so $S = |P|$ for the conditions under which the equation (1) holds.

Note, the formula (1) relates a group of three functions, each derived from the same original $f(x)$. The mathematical operations that need to be performed on the $f(x)$ in order for it to be used in (1) are all easily accomplished numerically, and therefore any real-life dataset can be readily used in place of $f(x)$ in the formula. If it holds, then such dataset must be continuous and smooth, and, by the same token, deterministic rather than random. Consequently, if an aperiodic (oscillatory) time series yields $S = |P|$ from formula (1), then such a time series must be chaotic rather than stochastic.

We, therefore, want to use formula (1) as a diagnostic tool to find out whether the aperiodic calorimetric time series shown in Figures 2 and 3 are deterministic, i.e., representing an occurrence of mathematical chaos in the kinetics of the $O_2 + H_2$ recombination, or stochastic, i.e., only fluctuating randomly.

However, the S and P may be considered equal only within a numerical error, and for the real-life data, the S and P may also be affected by an experimental error, so in practice the two reals may be only approximately equal, even for the datasets for which formula (1) holds. To account for this, and still be able to use formula (1) diagnostically, we define the absolute relative difference (ARD) of S and P according to the following formula:

$$D = \left| \frac{S - |P|}{0.5(S + |P|)} \right| = 2 \left| \frac{R - 1}{R + 1} \right|, \quad (2)$$

where $R = S/|P|$. We note that $D \rightarrow 0$ as $R \rightarrow 1$, and $D \rightarrow 2$ as $R \rightarrow \infty$, or $R \rightarrow 0$. Thus the D -test yields a real number $D \in [0, 2]$, for any dataset, independent of its size and kind of data included. As a diagnostic measure, the D will be close to zero for the continuous and smooth, and hence deterministic datasets, i.e., for $S \approx P$. Conversely, the more disparate the values of S and $-P$, the closer the D values will be approaching two.

The D -values scored by the calorimetric datasets represented in Figures 2 and 3 are listed in Table 1. For the reader's convenience, the D -scores are also marked for each calorimetric curve in Figures 2 and 3. The values for the 6.2 % rounds in both figures can serve as a reference, since these rounds featured no oscillations, and the calorimetric curves recorded for them are therefore certainly deterministic. The highest obtained score of $D = 0.0018849$ is for the 8.6 % round in Figure 2, which is by an order of magnitude higher than the $D = 0.00016344$ found for the 6.2 % round in the same experiment. The other aperiodic curves, however, scored similar to those in the 6.2 % rounds. For comparison, the D -values reported in Ref. 29 for random databases such as a sequence of 3,000 digits of π , and a random Fibonacci sequence were, respectively, 0.24783 and 1.0138, while on the other hand, a classic example of Lorenz chaos scored 0.0060459 in D . In the same article, the D -scores for the thermokinetic oscillations in sorption of hydrogen or deuterium in metallic palladium have been reported to be 0.00060501, 0.0010340 and 0.003041 for the periodic, quasiperiodic and chaotic oscillations respectively.²⁹ Hence, the score for the 8.6 % round in Figure 2 remains well within a range expected for determinism meaning that oscillations in this round are chaotic. It can be therefore concluded, that the aperiodic oscillations observed in the recombination of $H_2 + O_2$ in Figures 2 and 3 are all manifestation of mathematical chaos in the process kinetics.

Table 1. The results of the *D*-test for determinism in the calorimetric time series represented in Figures 2 and 3.

Concentration of H ₂ , % vol.	Dynamics of oscillations	<i>D</i>	<i>S</i>	<i>P</i>
6.2 (Fig.2)	nonoscillatory	0.00016344	1.5787e+07	-1.5784e+07
7.2 (Fig.2)	periodic and aperiodic	0.00015023	2.2501e+07	-2.2497e+07
8.6 (Fig.2)	aperiodic	0.0018849	6.7358e+07	-6.7231e+07
6.2 (Fig.3)	nonoscillatory	0.00013286	2.5894e+07	-2.5890e+07
7.2 (Fig.3)	quasiperiodic and periodic	0.00032756	3.8374e+07	-3.8362e+07
8.6 (Fig.3)	aperiodic	0.00017853	7.1165e+07	-7.1152e+07

3.3. Anomalous differential heats of the H₂ + O₂ recombination reaction. Figure 5 compares the differential heats of process and the conversions of hydrogen in the H₂ + O₂ recombination, both plotted as a function of time for individual rounds shown in Figure 3. The differential heats of process are calculated by pointwise division of the calorimetric curve by the curve of rate of hydrogen uptake. Figure 5A depicts the data for the nonoscillatory 6.2 % round in Figure 3, and it shows that the differential heat of the process (green line) remains nearly constant, albeit slightly increasing, throughout the whole round, running close to the 250 kJ/mol H₂ level corresponding to the heat of water formation. The conversion (magenta line) decreases slowly from initial 100 % H₂ to ca. 90 % H₂ after 1 h of experiment. Similar degrees of the H₂ conversion has been also obtained in our experiments with a larger reactor, using 0.5 cm³ samples of the Pd/Al₂O₃ catalysts, under similar reaction conditions, except for the H₂ concentration which was lowered to 0.5 % vol. for safety reasons.³⁷

Figures 5B, C, E and F represent data obtained at higher H_2 concentration in reaction mixture, namely 7.2 %vol. (i.e., the 7.2 % round). Figure 5B shows the curves of differential heat (green) and conversion (magenta) for the whole 7.2 % round. After a relatively “quiet” period of initial 1500 s, the outburst of strong oscillations appears spontaneously, lasting for ca. 500 s, followed by a period of chaotic oscillations nearing the end of the round. In both the initial and the concluding period, the differential heat stays close to ca. 300 kJ/mol H_2 , with the conversion ranging from ca. 90 % H_2 to 80 % H_2 .

Figure 5C shows an enlargement of a fragment representing the outburst of quasiperiodic oscillations. The two time series, the differential heat of process and the conversion of hydrogen, are precisely anti-phase synchronized, with the drops in conversion inversely proportional to the amplitude of differential heat. The differential heat of the $H_2 + O_2$ recombination reaches as high as ca. 700 kJ/mol H_2 at the crests, which is nearly three times as much as the heat of water formation of 242 kJ/mol H_2 .

The differential heat reaching 700 kJ/mol H_2 can also be seen in Figure 5D showing the data for the 8.6 % round. Here the outburst of seemingly periodic oscillations of large amplitude only lasts for an initial 400s, followed by chaotic oscillations continuing to the end of the round at an average level of roughly 300 kJ/mol H_2 , occasionally reaching 400 kJ/mol H_2 . In the initial outburst, the differential heat oscillations are anti-phase synchronized with the oscillations in conversion of hydrogen, after which the hydrogen conversion continues oscillating slightly at a level of ca 90 %.

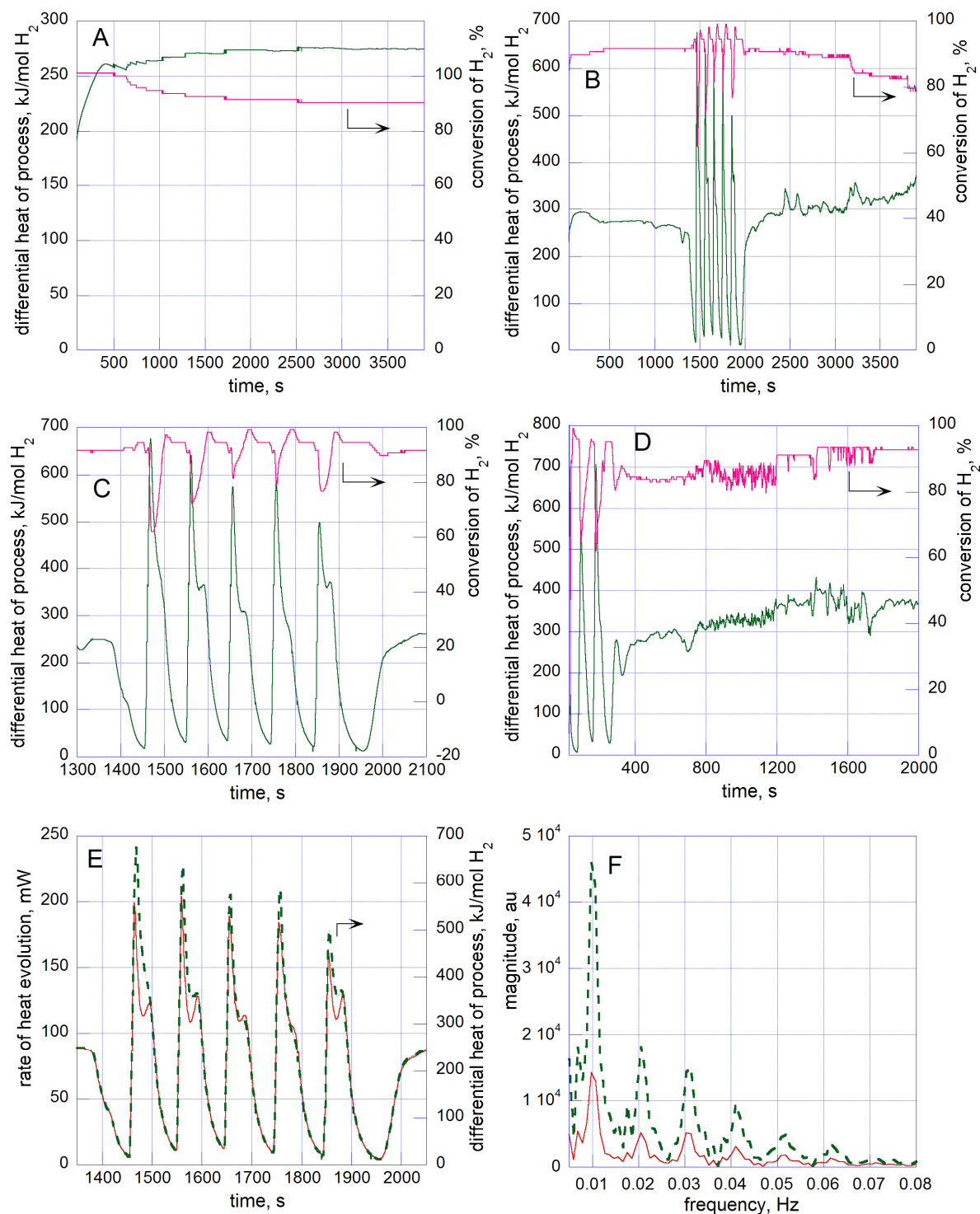


Figure 5. A-D: the differential heat of process (green) compared to the conversion of H_2 (magenta) calculated for data in Figure 3, for individual H_2 concentrations: 6.2 % H_2 (A), 7.2 % H_2 (B, C) and 8.6 % H_2 (D). Panel C shows an expansion of the large-amplitude oscillations

from Panel B. Panel E shows that the quasiperiodic character of these oscillations is strictly conserved when the original rate of heat evolution (red solid) is recalculated into differential heat of process (green dashed). Panel F shows power spectra for the time series in Panel E, with corresponding colors. Two incommensurate frequencies indicate quasiperiodic dynamics.

Figure 5E compares the original calorimetric curve (solid red), representing the rate of heat evolution against time, to the curve of differential heat of process (dashed green). It shows that the oscillations in differential heat of process strictly preserve the dynamic character as well as the frequencies of the original thermokinetic oscillations. Hence, the mathematical operation on two experimental time series, that is, the pointwise division of the calorimetric curve by the TCD curve, did not introduce any distortion to the frequency of resulting time series representing the differential heat of process. The power spectra in Figure 5F confirm that the original calorimetric curve and the curve of differential heat of process both show the same quasiperiodic dynamics, having the same frequencies.

3.4. High thermal effects in calorimetric oxygen titration. *3.4.1. Overview.* The calorimetric oxygen titration measures thermal effects of small pulses of O₂ on hydrogen-saturated catalysts.^{31,32} This method resembles the oxygen titration in that after initial treatment with hydrogen the sample is repeatedly exposed to pulses of gaseous oxygen, but the measured quantity is the heat evolution accompanying the ensuing water formation. Unlike the commonly used oxygen titration method, the amounts of oxygen being consumed are not determined in the calorimetric “version” of this method. A strictly controlled volume of oxygen for each pulse is achieved by using gas loop as a dosing device, and each pulse is recorded as a separate exothermic peak with gas flow-through microcalorimeter. The *in situ* calibration procedure

makes it possible to determine instantly the amounts of heat represented by each peak. For individual pulses, therefore, the resulting molar heat can be readily evaluated, as a ratio of the evolved heat and the number of moles of O_2 in a pulse volume, assuming that the latter is totally consumed. A typical saturation/oxidation cycle is therefore a two-step procedure in which a period of $H_2(D_2)$ saturation is followed by a sequence of pulses of oxygen (typically $0.09 \mu\text{mol}$), with the dosing continued until a heat evolution is no longer detected, after which the sample is ready for the next saturation/oxidation cycle to be initiated. The cycles can be repeated on the same sample practically indefinitely. Typically, the calorimetric oxygen titration experiment consists of several saturation/oxidation cycles repeated one by one, with thermal effects of both the oxidation pulses as well as of the hydrogen-saturations being measured.

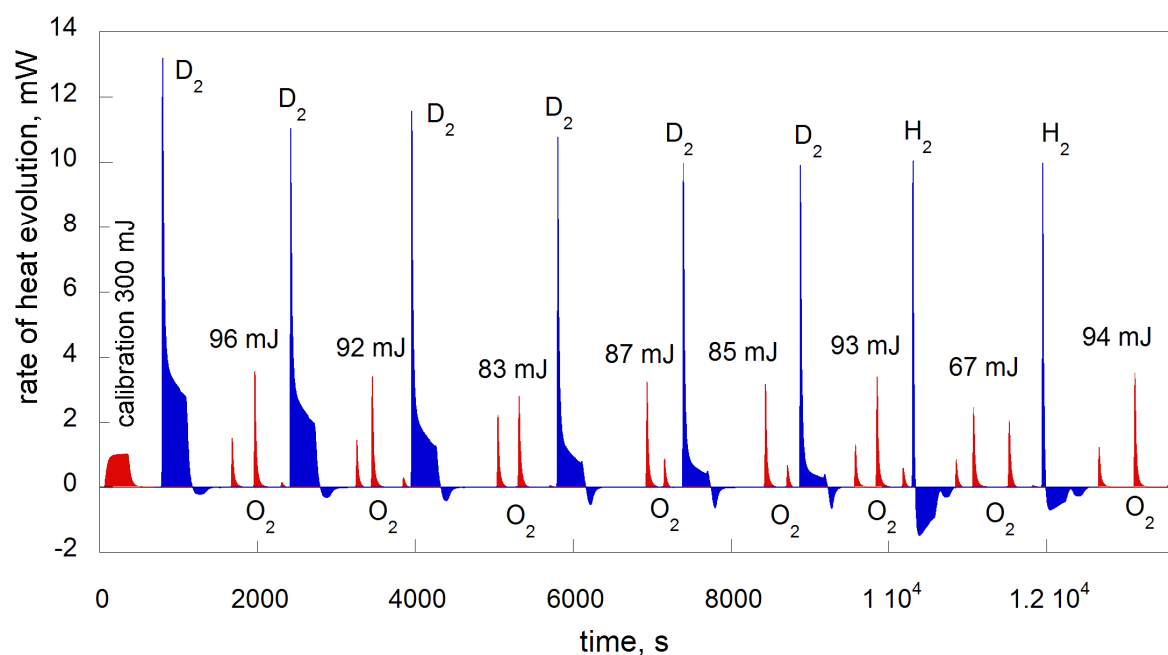


Figure 6. Calorimetric oxygen titration: a sequence of saturation/oxidation cycles for the 2%Pd/Al₂O₃ catalyst. The red peaks represent the heat evolution produced by $0.09 \mu\text{mol } O_2$ pulses, each series following a blue peak representing the heat evolution in saturation with either H_2 or D_2 .

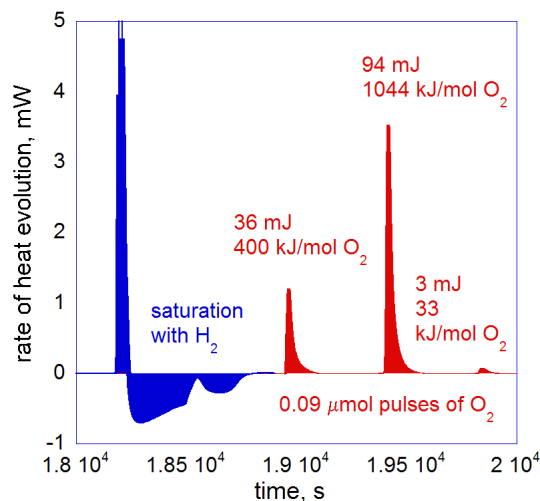


Figure 7. The last saturation/oxidation cycle in Figure 6 expanded.

3.4.2. 2%Pd/Al₂O₃ catalyst. Figure 6 represents a succession of saturation/oxidation cycles repeated eight times (during a one-day experimental session) using a 0.0756 g sample of 2%Pd/Al₂O₃ catalyst, under normal conditions of temperature and pressure. Using synthetic air (20 % O₂ + 80 % N₂) as source of oxygen and a 10 mm³ gas loop as dosing device affords 0.09 μmol pulses of O₂, with N₂ being used as the carrier gas. Small red peaks represent the pulses of oxygen, coming in short sequences of two or three, each sequence following a larger blue feature representing a 5 min period of catalyst saturation with hydrogen or deuterium. Figure 7 shows an example of a single saturation/oxidation cycle, the last of those shown in Figure 6. The area under each red peak represents the thermal effect of a 0.09 μmol pulse of oxygen reacting with the hydrogen-saturated catalyst. Division of the thermal effect by the number of moles of O₂ (i.e., 0.09 μmol) yields the molar heat of oxygen consumption for each pulse. Thus in Figure 7, the three pulses yielded successively 400 kJ/mol O₂, 1044 kJ/mol O₂ and 33 kJ/mol O₂. The molar heat evolved in the second pulse is the highest, and, strikingly, it is exceeding the heat of water formation (484 kJ/mol O₂) by a factor of two. For clarity, only the thermal effects of the

highest peaks in each sequence of oxygen pulses are marked in Figure 6. The molar heats for these highest peaks range from 1066 kJ/mol O₂ to 744 kJ/mol O₂ (i.e., from 533 kJ/mol H₂ to 372 kJ/mol H₂), each of them considerably higher than the heat of water formation.

The histogram in Figure 8 compiles the thermal effects of the highest peaks from the entirety of seventeen saturation/oxidation cycles carried out on the 2%Pd/Al₂O₃ catalyst (over several days), under ambient conditions, using either H₂ or D₂ for catalyst saturation prior to oxygen exposures. Thus the green and red bars represent the 0.09 μmol O₂ pulses following either the H₂- or the D₂-saturation, respectively. The bars have been arranged arbitrarily in a descending order to facilitate visual examination, irrespective of their isotopic origin. It can be concluded, that the hydrogen isotope use for saturation of catalyst has no effect on the heights of anomalous thermal effects that are recorded on pulses of O₂. Most of these effects are around 1000 kJ/mol O₂, i.e., twice of the heat of water formation, the level marked by the thin dashed line in the histogram in Figure 8.

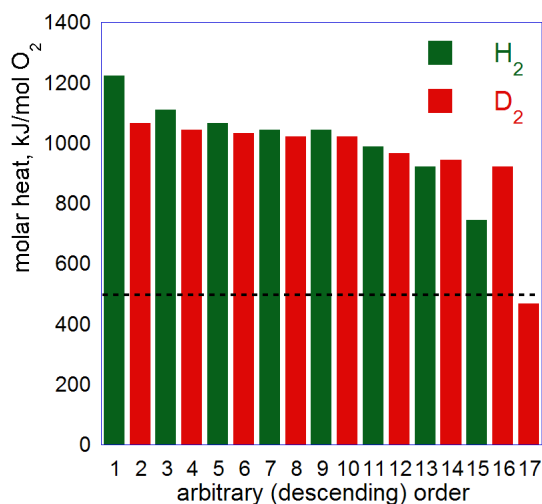


Figure 8. The highest thermal effects extracted from several hydrogen (deuterium)-saturation/oxidation cycles for the 2%Pd/Al₂O₃, using pulses of 0.09 μmol O₂. The dotted line at 484 kJ/mol O₂ marks the level corresponding to the standard molar heat of water formation.

1
2
3
4
5
6 It should be stressed, that the anomalously high exothermic effects observed in the oxygen
7 titration cannot be attributed to any systematic overestimation error. In fact, the opposite may be
8 the case: the estimates can be downward-biased, if the consumption of an O₂ pulse is only partial
9 rather than total as assumed. In such case, the thermal effect recorded for a pulse arises from an
10 amount of oxygen less than the nominal amount of 0.09 μmol actually taken for calculation,
11 which can only underestimate the molar heat so evaluated.
12
13
14
15
16
17
18

19
20 It is interesting to notice that the shapes of hydrogen-saturation (blue) peaks in Figure 6 vary
21 continually from one blue peak to the next, with the exothermic component of the peak
22 decreasing and the endothermic part becoming more pronounced. This seems to be a result of a
23 growing deposit of water formed on the catalyst surface during the oxygen exposures. These
24 surface-bound water molecules are then partially replaced each time the sample is saturated by
25 hydrogen (deuterium). The first saturation/oxidation cycle starts with a fresh and relatively
26 water free catalyst, giving rise to predominantly exothermic effect of hydrogen sorption, but a
27 small endothermic feature likely resulting from the water desorption can also be noticed. As
28 successive O₂ pulses causes the water deposit to grow, more and more water appears to desorb
29 leading to gradual increase of the endothermic part in each successive saturation.
30
31
32
33
34
35
36
37
38
39
40
41
42

43 *3.4.3. 5%Pd/Al₂O₃ catalyst.* Tables 2 shows the results of calorimetric oxygen titration with a
44 0.1129 g sample of the commercial 5%Pd/γ-Al₂O₃ catalyst. The data in Table 2 have been
45 obtained using the same model of FMC microcalorimeter, but it was physically different
46 instrument, at different location and run by different group of co-authors, in order to test an
47 “inter-instrumental” reproducibility of our results. Two saturation/oxidation cycles are
48 represented. They differ in the duration of hydrogen saturation period, which was respectively 6
49
50
51
52
53
54
55
56
57
58
59
60

min and 1 min. In each cycle, the exposure to a series of 0.09 μmol pulses of oxygen started 30 min after the completion of saturation, the injections being made at 10 min intervals. A total of respectively 8 and 7 pulses of O_2 have been made in each cycle before an injection no longer resulted in the evolution of heat. The molar heat per pulse ranges from 533 kJ/mol O_2 to 1056 kJ/mol O_2 , and from 478 kJ/mol O_2 to 1067 kJ/mol O_2 , in the first and the second saturation/oxidation cycle respectively. It can be noticed that a majority of the O_2 injections give rise to energies that are significantly above that of the combustion of H_2 . Hence, the magnitude of the anomalous effect, i.e., an extent to which the molar heat obtained for each O_2 pulse exceeds that of water formation reaches a factor of two, irrespective of duration of the saturation of sample with hydrogen.

With anomalously high thermal effects occurring in certain pulses, it seems that the total heat evolution for all pulses within a cycle remains constant if represented relative to the Pd mass. Summation over heats of pulses in individual cycles listed in Table 2 yields the totals of 577 mJ and 535 mJ, respectively in the first and the second cycle, corresponding to 0.1022 kJ/g Pd and 0.0951 kJ/g Pd. A similar summation for 2%Pd/ Al_2O_3 in Figure 6 yields the totals for individual sequences of O_2 pulses ranging from 133 mJ to 151 mJ, and an average heat of 0.0951 kJ/g Pd. Hence, practically the same total heat per gram Pd, ca. 0.1 kJ/g Pd, has been observed in the calorimetric oxygen titration for two catalysts with different Pd loadings, i.e., 2% Pd and 5 % Pd.

Table 2. Thermal effects of pulses of O₂ on commercial 5%Pd/Al₂O₃ catalyst.

O ₂ Injection No.	Individual energy of peak, mJ	Energy per mole, kJ/mol O ₂
first hydrogen-saturation/oxidation cycle (H₂ sat. for 6 min)		
1	48	533
2	47	522
3	60	667
4	76	844
5	89	989
6	95	1056
7	91	1011
8	71	789
second hydrogen-saturation/oxidation cycle (H₂ sat. for 1 min)		
1	43	478
2	54	600
3	78	867
4	81	900
5	94	1044
6	96	1067
7	89	989

3.4.4. 2%PdAu/Al₂O₃ catalyst. Figure 9 shows that increasing oxygen content in the titrating pulses volume may decrease or indeed eliminate the anomalous heat evolution which has been repeatedly observed on the same catalyst with the use of smaller 0.09 μmol pulses of O₂ under the same ambient conditions of temperature and pressure. Figure 9A shows a pair of two saturation/oxidation cycles using the 0.09 μmol pulses of O₂ on a 0.0962 g sample of bimetallic

2%PdAu/Al₂O₃ catalyst. On the other hand, Figure 9B represents another pair of two cycles, in which using pure oxygen instead of synthetic air in the same 10 mm³ dosing volume affords pulses of 0.46 μmol O₂, with N₂ still used as the carrier, and with the same catalyst. Clearly, the small pulses produced much higher energy per mole, with the highest effects of 1100 kJ/mol O₂ and 944 kJ/mol O₂ respectively for the two cycles represented in Figure 9A, both exceeding the heat of water formation by a factor of around two. The effects are practically identical to those obtained for the monometallic 2%Pd/Al₂O₃ using the 0.09 μmol pulses of O₂ (cf. Fig. 7). On the other hand, the molar heats yielded by the 0.046 μmol O₂ pulses under the same conditions (Fig. 9B) are respectively 522 kJ/mol O₂ and 549 kJ/mol O₂, both only marginally higher than the thermodynamic value expected for the water formation. Similar effects of increasing oxygen content leading to molar heats less excessive, but still firmly above 484 kJ/mol O₂ have also been observed with another bimetallic catalyst, namely 1%PdPt/Al₂O₃, in which case the calorimetric titration yielded ca. 1100 kJ/mol O₂ for the 0.09 μmol O₂ pulses, compared to ca. 850 kJ/mol O₂ for the 0.46 μmol O₂ pulses (figures not shown). The total heats yielded by all the O₂ pulses per individual cycles in Figure 9A are 216 mJ and 203 mJ, corresponding to 0.1039 kJ/g Pd+Au and 0.1055 kJ/g Pd+Au respectively, i.e., practically the same for both cycles.

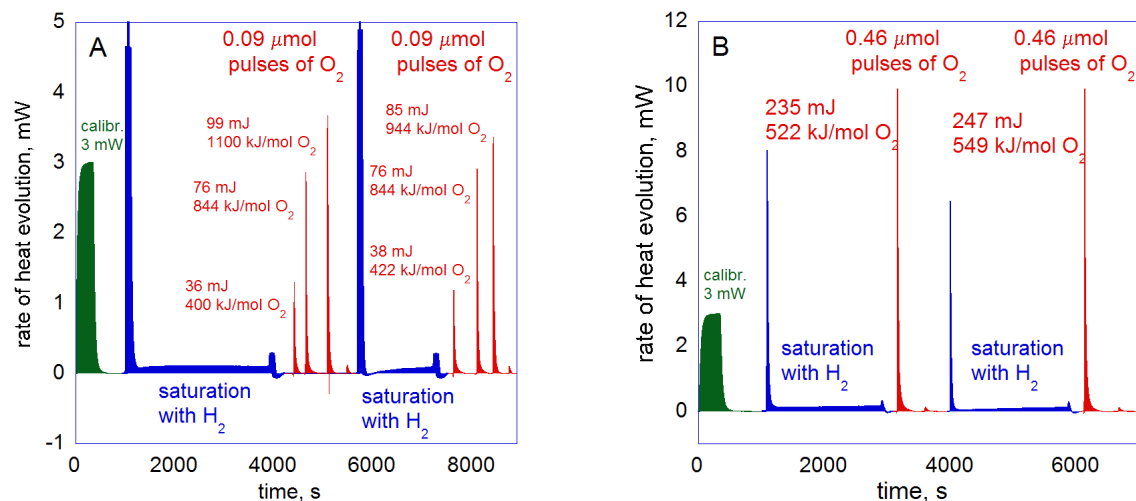


Figure 9. Calorimetric oxygen titration of the 2%PdAu/Al₂O₃ using pulses of O₂ of different sizes: 0.09 μmol (A), and 0.46 μmol (B). A pair of successive hydrogen-saturation/oxidation cycles is shown in each figure.

4. DISCUSSION

4.1. Origin of nonlinearity and chaos. The chaotic, low-amplitude oscillations that can be seen in Figure 5B and D, are likely to reflect the nonlinear phenomena in the H₂ + O₂ reaction mechanism. A possible origin of nonlinearity in oxidation of hydrogen on the Pt(111) surface has been discussed in Ref. 38. Accordingly, the nonlinear aspect is provided by a step in reaction network on Pt(111) that consists of the reaction of atomic oxygen species with the adsorbed H₂O, i.e., O_{ad} + H₂O_{ad} → 2OH_{ad}. Separate areas on the Pt surface covered to various extents by the reacting species (O_{ad}, H₂O_{ad}, OH_{ad}) have been observed moving along the catalytic surface in time resolved experiments, video recorded in situ using STM, nevertheless, the hydrogen species could not be observed.³⁸ This reaction may expectedly occur on the palladium surface as well as on the Pt(111). We reiterate that a possibility of chaos in the oxidation of

hydrogen has been predicted by mathematical modeling.^{39,40} Experimentally, chaos in hydrogen oxidation has been observed in the electrochemical oxidation of hydrogen on a platinum anode in the presence of copper ions,⁴¹ and in the oxidation of H₂ on Ni.¹⁷ We are not aware of experimental evidence of chaos in H₂/O₂/Pd system published as yet, although aperiodic oscillations in oxidation of hydrogen on Pd wire have been reported.⁸

4.2. The role of atomic hydrogen. The results of calorimetric oxygen titration suggest that the total heat produced by a sequence of O₂ pulses following the hydrogen-saturation is on average the same if represented relative to the Pd mass in the sample of catalyst used. Thus it was ca. 0.1 kJ/g Pd for both the 2%Pd/Al₂O₃ and the 5%Pd/Al₂O₃ catalyst, and 0.1 kJ/g Pd+Au for the 2%PdAu/Al₂O₃. This makes it possible to estimate, however crudely, the H/Pd atomic ratio for each catalyst under study. For the 2%Pd/Al₂O₃, Figure 6 shows that each saturation/oxidation cycle uses three pulses of O₂ to deplete the pre-sorbed hydrogen on the 0.0756 g sample containing ca. 14 μgramatom Pd. The total amount of oxygen introduced in each cycle is $3 \times 0.09 = 0.27$ μmol O₂, potentially requiring 1.08 μgramatom of H to form 0.54 μmol H₂O. The estimated H/Pd ratio for 2%Pd/Al₂O₃ is therefore $1.08/14 = 0.08$. The 0.0962 g sample of 2%PdAu/Al₂O₃ with the Pd/Au ratio of ca. 7/3 (cf. Fig. 1), contains ca. 10.1 μgramatom Pd and 4.2 μgramatom Au. In this case it took around 0.36 μmol O₂ (four 0.09 μmol pulses; cf. Fig. 9) for the sample to be depleted of hydrogen, corresponding to 1.44 μgramatom of atomic H, yielding the H/Pd ratio of $1.44/10.1 = 0.14$, or the H/(Pd + Au) ratio of $1.44/(10.1 + 4.2) = 0.1$, and for the 5%Pd/Al₂O₃ catalyst the H/Pd ratio so calculated is 0.05. These relatively low H/Pd ratios may be rationalized in two ways. The first would assume that only a most active minority of the hydrogen species sorbed in the metal particles gives rise to the heat evolution measured in the calorimetric oxygen titration. The second may suggest that sorption of hydrogen

in the studied catalysts is limited only to the metal particles surface. The latter is likely to be the case for the 2%PdAu/Al₂O₃ catalyst, with the metal particles each containing ca. 30 atomic % Au, which is a high enough content to prevent any significant sorption of hydrogen in the bulk of such PdAu alloy particles.⁴² For both the Pd/Al₂O₃ materials, however, it cannot be excluded that their Pd particles do contain both the bulk-absorbed and the surface-adsorbed hydrogen species, but only a fraction is active in the oxygen titration. It may be related to a phenomenon of enhanced chemical stability, reported for hydrogen species “trapped” inside the 6.1 nm Pd particles,⁴³ or inside the Pd nanocrystals supported on Al₂O₃.⁴⁴ It is possible that this enhanced stability of hydrogen species sorbed in the bulk of the Pd particles effectively prevents them from reacting with oxygen pulses rapidly dosed in the titration method. Thus the abnormally high thermal effects of around 1000 kJ/mol O₂ (500 kJ/mol H₂, exceeding twice the heat of water formation) obtained in the oxygen injections arise from the interaction of oxygen with only a fraction of most energetic hydrogen species present within the metallic particles. This is in agreement with the results of Figure 9B showing that the saturation/oxidation cycles using larger pulses of O₂ injected on the 2%PdAu/Al₂O₃, failed to produce the unusually high thermal effect on this catalyst. Instead, the thermal effects of the 0.46 μmol O₂ pulses are only marginally higher than the 484 kJ/mol O₂, as though for the larger partial pressures of O₂ the anomalous exothermic effects were obscured by the standard thermal effect accompanying the dominant reaction of water formation. A similar conclusion, concerning the possibility for only a fraction of the H-species to constitute the most active minority, has been reached in Ref. 45 for the case of a Ni metal catalyst. Accordingly, the fortuitous fraction of most active hydrogen species that are actually involved in hydrogenation processes on metallic Ni catalyst are those H-species that are freshly emerging from the nickel subsurface layer.

1
2
3 In contrast to the titration method, hydrogen and oxygen are both continuously fed into the
4 microcalorimetric cell in the flow recombination experiments on the 2%Pd/Al₂O₃ catalyst (Figs.
5
6
7
8 2 and 3). Here, the ambiguous role of hydrogen seems to be further underlined by the way that
9
10 the hydrogen uptake rate and the rate of heat evolution are anti-phase synchronized during
11
12 quasiperiodic oscillations. Surprisingly, the tops of heat evolution coincide with the dips of
13
14 hydrogen uptake (Figs. 4A and B), whereas what should be expected is rather the opposite. In
15
16 fact, it seems reasonable to assume that acceleration in heat evolution should be accompanied by
17
18 a corresponding increase in hydrogen uptake, if the rate of heat production reflects the rate of
19
20 hydrogen oxidation. Instead, however, the maxima of heat production are accompanied by
21
22 decreases of hydrogen consumption. The differential heat of recombination process reaches as
23
24 high as 700 kJ/mol H₂ (Figs. 5B, C and D) which is nearly three times as much as the heat of
25
26 gaseous water formation from elements (242 kJ/mol H₂). This seems to suggest that yet another
27
28 hydrogen-involving process, rather than the water formation, but even more energetic, may be
29
30 occasionally outbursting and resulting in the anomalously high heat production.
31
32
33
34
35

36 It is difficult to explain the heat evolution as high as the instantaneous 700 kJ/mol H₂.
37
38 Compared to the heat of H₂O_g formation it is higher by ca. 450 kJ/mol H₂. The outstanding
39
40 value is close to the bond energy in the H₂ molecule of 436 kJ/mol H₂,⁴⁶ which might be
41
42 implying that the large thermal effect results from oxidation of atomic H species, rather than
43
44 molecular H₂. The enthalpy of reaction involving molecular O₂ and the atomic H species, 1/2O₂
45
46 + 2H → H₂O, would be $\Delta H = -(242 + 436) = -678$ kJ/mol H₂ (cf. Table S1 in Supporting
47
48 Information file), which is comparable to the figure of 700 kJ/mol H₂ actually observed.
49
50 However, a hypothetical presence of a substantial quantity of free hydrogen atoms on the
51
52 Pd/Al₂O₃ catalyst would have required its own explanation. The energy needed to dissociate the
53
54
55
56
57
58
59
60

H₂ molecule to form two free hydrogen atoms is large, 436 kJ/mol H₂, and presumably, such expenditure should be somehow reflected in the microcalorimetric experiments in a form of large endothermic effects, which however are not observed. On the contrary, Figures 6 and 9 show, that the thermal effects accompanying saturation of catalyst with hydrogen or deuterium are actually mostly exothermic. Therefore, the sorbed hydrogen species that are formed on the 2%Pd/Al₂O₃ catalyst, although resulting from dissociative adsorption on metallic Pd, must be energetically very different from the free H atoms.

There is currently no satisfactory explanation for the abnormally high thermal effects in the H₂ + O₂ recombination reported here, but it may be suggested that the hydrogen-related anomalous heat evolutions may be falling into the same category with the low energy nuclear reaction phenomena (LENR). In view of the fact, that the PARs are intended to be used in nuclear reactors as crucial safety devices, a possibility of uncontrollable heat evolutions caused by these very devices themselves calls for a special consideration.

4.3. A danger of LENR occurrence. It is usual to view the low energy nuclear reactions (LENR) as a revolutionary new energy source, but they may also be viewed as posing a danger, threatening a sudden emission of large thermal energy, in case of their unexpected occurrence. Here by the LENR we understand the phenomena of extraordinary high thermal effects first reported by Fleischmann and Pons.⁴⁷ It should be stressed that LENR seems to be related to the formation of atomic hydrogen (or deuterium) species. The actual nuclear character of the phenomena has never been conclusively confirmed however. Nevertheless, it seems to be well established now, that abnormally high heat evolutions do occasionally accompany the interactions in which the atomic hydrogen is involved. In our discussion here, we also consider the concept of the hydrino formation,⁴⁸ which technically is not considered a LENR

phenomenon, but it seems to fall into the same category of processes producing enormously high thermal effects, too large to be of chemical origin, at the presence of atomic hydrogen.

Apart from hydrogen, the LENR systems usually involve the metals like Pd and Ni, supported or otherwise, which are also well known as catalysts for hydrogen processes, where their ability for dissociative sorption of H_2 is conducive to their catalytic activity. Therefore, the supported Pd metal catalysts that are used in the PAR technology are in fact this sort of materials on which a LENR process may potentially occur. The recombination of H_2 involves molecular oxygen, and oxygen is not typically considered a component of LENR systems, but the difference may not be essential. There are reported experiments in which gaseous O_2 is present in the LENR process environment. This has been reported for the test of the prototype of the E-cat equipment. The process was run under high pressure of 25 bar but the authors explicitly state that the residual air has not been removed from the reaction chamber before loading it with hydrogen, and so it remains in the reacting space as “an impurity” throughout the process.⁴⁹ In addition, a patent has recently been granted for LENR-based a piston engine⁵⁰ in which oxygen is claimed to be a catalyst.

The LENR may be a promising energy source for the future, only provided they are understood and controllable. Anticipating availability of the technology, recently a report has been published by NASA⁵¹ describing novel constructions of flying vehicles specifically designed to be powered by LENR based engines. This is in spite of still unknown nature of the LENR phenomena, which the report admits is largely ill understood. In view of this ignorance, it seems prudent to concede that there may also exist a hazard of unexpected LENR occurrence in the industrial processes involving metals like Pd and the atomic hydrogen, potentially releasing uncontrollable amounts of energy. Here the PAR technology seems to be a case in point. In

fact, the possibility for certain accidents, that actually had happened in a nuclear plant, to be put down to a LENR or hydrino related explosion has been pointed out hypothetically.⁵² In view of a recent development of the technology of modular nuclear reactors, the threat of using PARs may be even aggravated by the fact that the modular reactors lack the large confinement and shielding of the traditional large constructions.

5. CONCLUSIONS

Thermokinetic oscillations in the process of oxidation of hydrogen on Pd-based catalysts have been recorded and the occurrence of mathematical chaos confirmed in the process. It has been shown that outbursts of quasiperiodic oscillations of large amplitude may occur spontaneously, but may also be triggered by a slight change in hydrogen concentration in the $H_2 + O_2$ reaction mixture. Anomalous heat evolutions reaching 700 kJ/mol H_2 in the outburst of quasiperiodic oscillations have been recorded. Thermal effects twice as much as the heat of water formation have been observed in the calorimetric oxygen titration of various Pd/ Al_2O_3 catalysts following their saturation with either hydrogen or deuterium, but no evidence of isotope effects has been found. For the PAR designing, this seems to suggest that a possibility of thermal effects much larger than that resulting from the standard thermodynamical value for the gaseous water formation of 242 kJ/mol H_2 should be taken into consideration. The fact that these high thermal effects may appear spontaneously and abruptly might be a source of unexpected threats posed by the PAR reactor itself.

AUTHOR INFORMATION

Corresponding author

*E-mail: nclalik@cyf-kr.edu.pl

ACKNOWLEDGEMENT

Financial support under Research task No SP/J/7/170071/12 “Study of hydrogen generation process in nuclear reactors under regular operation conditions and in emergency cases” financed by National Research and Development Center, Poland is gratefully acknowledged.

Supporting Information Available: Thermal effects of the gaseous water formation from elements for various combinations of molecular and atomic reagents. This material is available free of charge via the Internet at <http://pubs.acs.org>.

REFERENCES

- (1) Bachellerie, E.; Arnould, F.; Auglaire, M.; de Boeck, B.; Braillard, O.; Eckardt, B.; Ferroni, F.; Moffett, R. Generic approach for designing and implementing a passive autocatalytic recombiner PAR-system in nuclear power plant containments. *Nucl. Eng. Des.* **2003**, *221*, 151.
- (2) Deng, J.; Cao, X. W. A study on evaluating a passive autocatalytic recombiner PAR-system in the PWR large-dry containment. *Nucl. Eng. Des.* **2008**, *238*, 2554.
- (3) Reinecke, E. A.; Bentaib, A.; Kelm, S.; Jahn, W.; Meynet, N.; Caroli, C. Open issues in the applicability of recombiner experiments and modeling to reactor simulations. *Progress in Nuclear Energy*, **2010**, *52*, 136.

(4) Payot, F.; Ernst-Arndt Reinecke, E. A.; Morfin, F.; Sabroux, J. C.; Meynet, N.; Bentaib, A.; March, P.; Zeyen, R. Understanding of the operation behavior of a Passive Autocatalytic Recombiner (PAR) for hydrogen mitigation in realistic containment conditions during a severe Light Water nuclear Reactor (LWR) accident. *Nucl. Eng. Des.* **2012**, *248*, 178.

(5) Cox, J. D.; Wagman, D. D.; Medvedev, V. A. *CODATA key values for thermodynamics*. In *CRC Handbook of Chemistry and Physics*, (Lide, D. R., Ed.), 85th ed.; CRC Press: Boca Raton, FL., 2004, p 5-2.

(6) Borescov, G. K. *Heterogeneous Catalysis*; Nova Science Publishers: New York, 2003, p. 140.

(7) Yablonskii, G. S.; Bykov, V. I.; Elokhin, V. I.; Gorban, A. N. *Kinetic Models of Catalytic Reactions*; Elsevier Science Publishers B.V.: Amsterdam, New York, 1991, p. 259.

(8) Rajagopalan, K.; Sheintuch, M.; Luss, D. Oscillatory states and slow activity changes during the oxidation of hydrogen by palladium. *Chem. Eng. Commun.* **1980**, *7*, 335.

(9) Rajagopalan, K., Luss, D. The influence of surface structure on the oscillations in the rate of hydrogen oxidation over palladium. *Chem. Eng. Sci.* **1983**, *38*, 473.

(10) Gorodetskii, V.; Block, J. H.; Drachsel, W. Isothermal oscillations of the hydrogen-oxidation reaction on platinum: investigations in the field electron and field ion microscope. *Appl. Surf. Sci.* **1994**, *76-77*, 129.

(11) Zuninga, J. E.; Luss, D. Kinetic oscillations during the isothermal oxidation of hydrogen on platinum wires. *J. Catal.* **1978**, *53*, 312.

- (12) Tsai, P. K.; Maple, M. B. Oscillatory oxidation of H₂ over a Pt catalyst. *J. Catal.* **1986**, *101*, 142.
- (13) Belyaev, V. D.; Slinko, M. M.; Timoshenko, V. I.; Slinko, M. G. Generation of autooscillations in the hydrogen oxidation reaction on nickel. *Kinet. Katal.* **1973**, *14*, 810 (in Russian).
- (14) Vohs, J. M.; Masel, R. I. Effects of feed temperature and composition on oscillations during hydrogen oxidation on nickel powder covered nickel foils. *Chem. Eng. Commun.* **1984**, *28*, 327.
- (15) Seebauer, E. G.; Vohs, J. M.; Masel, R. I. Effects of artificial protrusions of self-sustained thermal oscillations during hydrogen oxidation on nickel. *Ind. Eng. Chem. Fundamen.* **1984**, *23*, 19.
- (16) Kurtanjek, Z.; Sheintuch, M.; Luss, D. Reaction Rate Oscillations during the Oxidation of Hydrogen on Nickel. *Berichte der Bunsengesellschaft für physikalische Chemie* **1980**, *84*, 374.
- (17) Kurtanjek, Z.; Sheintuch, M.; Luss, D. Surface state and kinetic oscillations in the oxidation of hydrogen on nickel. *J. Catal.* **1980**, *66*, 11.
- (18) Arif, H.; Stoukides, M. Rate and oxygen activity oscillations during hydrogen oscillation on nickel films in CSTR. *Chem. Eng. Sci.* **1986**, *41*, 945.
- (19) Slin'ko, M. M.; Jaeger, N. I. *Oscillating Heterogeneous Catalytic Systems. In Studies in Surface Science and Catalysis*; Elsevier: Amsterdam, New York, 1994, p. 93.
- (20) Imbihl, R.; Ertl, G. Oscillatory kinetics in heterogeneous catalysis. *Chem. Rev.* **1995**, *95*, 697.

(21) Digilov, R.; Nekhamkina, O.; Sheintuch, M. Thermal imaging of breathing patterns during CO oxidation on Pd/glass cloth. *AIChE J.* **2004**, *50*, 163.

(22) Yuranov, I.; Kiwi-Minsker, L.; Slin'ko, M.; Kurkina, E.; Tolstunova, E. D.; Renken, A. Oscillatory behavior during CO oxidation over Pd supported on glass fibers: experimental study and mathematical modeling. *Chem. Eng. Sci.* **2000**, *55*, 2827.

(23) Ohlhoff, A.; Engel, H. Flow-mediated spatial coupling during CO oxidation on a palladium-supported catalyst in a continuous-flow reactor. *Catal. Today* **2001**, *70*, 359.

(24) Hendriksen, B. L. M.; Bobaru, S. C.; Frenken, J. W.M. Bistability and oscillations in CO oxidation studied with scanning tunneling microscopy inside a reactor. *Catal. Today* **2005**, *105*, 234.

(25) Pyatnitskii, Yu. I.; Filonenko, G. V. On the mechanism of auto-oscillations in CO hydrogenation on supported palladium catalysts. *React. Kinet. Catal. Lett.* **1991**, *44*, 499.

(26) Westerterp, R.; Bos, R.; Wijngaarden, R.; Kusters, W.; Martens, A. Selective Hydrogenation of Acetylene in an Ethylene Stream in an Adiabatic Reactor. *Chem. Eng. Technol.* **2002**, *25*, 529.

(27) Lalik, E.; Haber, J.; Groszek, A. J. Oscillatory Rates of Heat Evolution during Sorption of Hydrogen in Palladium. *J. Phys. Chem.* **2008**, *112*, 18483.

(28) Lalik, E. An empirical dependence of frequency in the oscillatory sorption of H₂ and D₂ in Pd on the first ionization potential of noble gases. *J. Chem. Phys.* **2011**, *135*, 064702.

(29) Lalik, E. Chaos in oscillatory sorption of hydrogen in palladium. *J. Math. Chem.* **2014**, *52*, 2183.

(30) Groszek, A. J.; Lalik, E.; Haber, J. Heats of interaction of hydrogen with gold and platinum powders and its effect on the subsequent adsorptions of oxygen and noble gases. *Appl. Surf. Sci.* **2010**, *256*, 5498.

(31) Groszek, A. J.; Lalik, E. Effect of oxygen on the production of abnormally high heats of interaction with hydrogen chemisorbed on gold. *Appl. Surf. Sci.* **2011**, *257*, 3192.

(32) Groszek, A. J. Abnormally high heat generation by transition metals interacting with hydrogen and oxygen molecules. *Adsorption* **2013**, *19*, 235.

(33) Kosydar, R.; Góral, M.; Gurgul, J.; Drelinkiewicz, A. The effect of support properties in the preparation of Pd size-controlled catalysts by “water-in-oil” microemulsion method. *Catal. Comm.* **2012**, *22*, 58.

(34) Szumelda, T.; Drelinkiewicz, A.; Kosydar, R.; Gurgul, J. Hydrogenation of cinnamaldehyde in the presence of PdAu/C catalysts prepared by the reverse “water-in-oil” microemulsion method. *Appl. Catal. A* **2014**, *487*, 1.

(35) Lalik, E.; Mirek, R.; Rakoczy, J.; Groszek, A. Microcalorimetric study of sorption of water and ethanol in zeolites 3A and 5A. *Catalysis Today* **2006**, *114*, 242.

(36) Veser, G. Experimental and theoretical investigation of H₂ oxidation in a high-temperature catalytic microreactor. *Chem. Eng. Sci.* **2001**, *56*, 1265.

(37) Lalik, E.; Kosydar, R.; Tokarz – Sobieraj, R.; Witko, M.; Szumelda, T.; Kołodziej, M.; Rojek, W.; Machej, T.; Drelinkiewicz, A. Humidity induced deactivation of Al₂O₃ and SiO₂ supported Pd, Pt, Pd-Pt catalysts in H₂ + O₂ recombination reaction: the catalytic, microcalorimetric and DFT studies. *Appl. Catal. A* **2015**, *501*, 27.

(38) Völkening, S.; Bedürftig, K.; Jacobi, K.; Wintterlin, J.; Ertl, G. Dual-Path Mechanism for Catalytic Oxidation of Hydrogen on Platinum Surfaces. *Phys. Rev. Lett.* **1999**, *83*, 2672.

(39) Chumakov, G. A.; Chumakova, N. A. Weakly Stable Dynamics in a Three-Dimensional Kinetic Model of Catalytic Hydrogen Oxidation. *Chemistry of Sustainable Development* **2003**, *11*, 63.

(40) Chumakov, G. A.; Chumakova, N. A. Modeling of Chaotic Dynamics in a Heterogeneous Catalytic Reaction. *AIP Conf. Proc.* **2009**, *1168*, 264.

(41) Krischer, K.; Lübke, M.; Wolf, W.; Eiswirth, M.; Ertl, G. Chaos and Interior Crisis in an Electrochemical Reaction. *Berichte der Bunsengesellschaft für physikalische Chemie* **1991**, *95*, 820.

(42) Kobayashi, H.; Yamauchi, M.; Ikeda, R.; Kitagawa, H. Atomic-level Pd–Au alloying and controllable hydrogen-absorption properties in size-controlled nanoparticles synthesized by hydrogen reduction. *Chem. Commun.* **2009**, 4806.

(43) Kobayashi, H.; Yamauchi, M.; Kitagawa, H.; Kubota, Y.; Kato, K.; Takata, M. On the Nature of Strong Hydrogen Atom Trapping Inside Pd Nanoparticles. *J. Am. Chem. Soc.* **2008**, *130*, 1828.

(44) Wilde, M.; Fukutani, K.; Naschitzki, M.; Freund, H. J. Hydrogen absorption in oxide-supported palladium nanocrystals. *Phys. Rev. B* **2008**, *77*, 113412.

(45) Ceyer, S. T. The Unique Chemistry of Hydrogen beneath the Surface: Catalytic Hydrogenation of Hydrocarbons. *Acc. Chem. Res.* **2001**, *34*, 737.

(46) Kerr, J. A. *Strengths of chemical bonds*. In *CRC Handbook of Chemistry and Physics*, (Lide, D. R., Ed.), 85th ed.; CRC Press: Boca Raton, FL., 2004, p 9-55.

(47) Fleischmann, M. and Pons, S. Electrochemically Induced Nuclear Fusion of Deuterium. *Journal of Electroanalytical Chemistry* **1989**, 261, 301.

(48) Phillips, J.; Mills, R. L.; Chen, X. Water bath calorimetric study of excess heat generation in “resonant transfer” plasmas. *J. Appl. Phys.* **2004**, 96, 3095.

(49) Essén, H.; Kullander, S. Experimental test of a mini-Rossi device at the Leonardocorp, Bologna 29 March 2011.

URL: <http://www.nyteknik.se/incoming/article3144960.ece/BINARY/Download+the+report+by+Kullander+and+Ess%C3%A9n+%28pdf%29>.

(50) Galindo Cabello, J. I.; Alvarez Lopez, J. Controlled nuclear fusion process, EP2026357, 2014.

(51) Wells, D. P. Low Energy Nuclear Reaction Aircraft, *NASA Aeronautics Research Institute* **2014**, URL: <http://ntrs.nasa.gov/archive/nasa/casi.ntrs.nasa.gov/20140010088.pdf>

(52) Yamamoto, H. Revisiting Anomalous Explosion of Hydrogen and Oxygen Mixture from a Viewpoint of Cold Fusion, JCF5, Japan CF - Research Society, Japan, 2003, p. 89.

(53) Kerr, J. A. *Strengths of chemical bonds*. In *CRC Handbook of Chemistry and Physics*, (Lide, D. R., Ed.), 85th ed.; CRC Press: Boca Raton, FL., 2004, p 9-56.

TOC figure

